

Dynamics of Skyrmion Collisions in 3+1 Dimensions

A. E. Alder, S. E. Koonin, R. Seki,^(a) and H. M. Sommermann^(b)

W. K. Kellogg Radiation Laboratory, California Institute of Technology, Pasadena, California 91125

(Received 19 August 1987)

We calculate classical skyrmion collisions in 3+1 dimensions. Numerical integration of Hamilton's equations for the chiral fields is based on a staggered leap-frog method. We study collisions of defensive hedgehog solitons at various impact parameters for center-of-mass energies of 157, 432, and 885 MeV. Internal excitations of the skyrmions and meson emission are observed. The time evolution of the pion field and momentum and baryon densities is shown, as are deflection functions and inelasticities. Some results for skyrmion-antiskyrmion annihilation are presented.

PACS numbers: 13.75.Cs, 11.10.Lm, 21.30.+y

Skyrme's model, which is recognized to have theoretical connections with QCD, provides a surprisingly successful description of baryon properties and the nucleon-nucleon interaction.¹ However, most calculations in the Skyrme model have been carried out for either static or adiabatic configurations with a variational product *Ansatz*, which has been shown numerically² to be unsatisfactory.

The full dynamics of the model embodies a unified description encompassing various nonlinear processes such as meson production, baryon excitation, and baryon pair production. Numerical evolution of the classical field equations can be useful in building intuition for the Skyrme model and can establish contacts with (and perhaps verify) the conventional static potential approach that employs adiabaticity assumptions. Also, since classical solutions are the essential foundation of any semiclassical approach, they might ultimately allow direct calculation of the *S* matrix, circumventing a potential description entirely. In this Letter, we report the first calculations of skyrmion collisions in 3+1 dimensions. A similar calculation has already been carried out³ with axial symmetry, effectively in two spatial dimensions.

The Lagrange density of the Skyrme model in Cartesian coordinates is

$$\mathcal{L} = -\frac{1}{8} F_\pi^2 (\partial_\mu \Phi_k)^2 - \frac{1}{4} e^{-2} (\partial_\mu \Phi_k)^2 (\partial_\nu \Phi_l)^2 + \frac{1}{4} e^{-2} (\partial_\mu \Phi_k \partial_\nu \Phi_l)^2, \quad (1)$$

where the chiral fields Φ_k are defined to form an SU(2) matrix $U = \Phi_0 + i\tau \cdot \Phi$, with $U=1$ at infinity. The equations of motion can be written as

$$\partial_t \Phi_k = M_{kl}^{(1)-1} \Pi_l, \quad (2a)$$

$$\partial_t \Pi_k = \nabla \cdot (M_{kl}^{(2)} \nabla \Phi_l), \quad (2b)$$

where Π_k are the canonical momenta $\delta\mathcal{L}/\delta(\partial_t \Phi_k)$. The symmetric 4×4 matrices $M^{(1)}$ and $M^{(2)}$ are given by

$$M_{kl}^{(1),(2)} = \frac{1}{4} F_\pi^2 \delta_{kl} + e^{-2} (\partial_a \Phi_m)^2 \delta_{kl} - e^{-2} (\partial_a \Phi_k) (\partial_a \Phi_l), \quad (3)$$

where $\alpha=1, 2, 3$ ($\alpha=0, 1, 2, 3$) in Eq. (3) defines $M^{(1)}$ ($M^{(2)}$).

We discretize the field equations in space on a uniform Cartesian lattice using lowest-order centered differences. The time integration is based on the staggered leap-frog method, an explicit scheme in which the fields at a time $t+\Delta t$ are given in terms of the known field variables at the previous times t and $t-\Delta t$. The time evolution proceeds through recurring updates of the field variables across the spatial lattice. Since the normalization of the chiral fields is not preserved by this process, we add a term of the form $\lambda \Phi_k \Phi_k$ to the Lagrange density.

The symmetries of the chiral fields in the cases we consider allow us to restrict the computation to one quadrant of the total space; boundary conditions at the interface introduce an image skyrmion that we need not treat explicitly. Our spatial lattice for this quadrant is $41 \times 41 \times 21$; with our lattice spacing $\Delta x = 0.084$ fm, this corresponds to $3.36 \times 3.36 \times 1.68$ fm³. Approximately 1500 time steps are needed to describe one complete scattering event, with Δt ranging from 0.007 to 0.003 fm/c, depending on the initial velocity. A measure of the numerical stability of the finite difference equations is the Courant condition, $\zeta \equiv c\Delta t/\Delta x \ll 1$; we use values of ζ between 0.075 and 0.013. Typical runs of our vectorized code on the National Magnetic Fusion Energy Computer Center Cray-2 or on the San Diego Supercomputer Center Cray XMP/48 take 30 central processing unit minutes.

In this work we focus on the scattering of defensive hedgehog skyrmions, although our code evolves an arbitrary field configuration. We construct our initial condition by applying Lorentz boosts to well separated static spherical solutions. The skyrmions translate uniformly before collision and we have no need for an artificial viscosity term³ to stabilize the calculation. Total energy and baryon number are calculated by centered finite-difference formulas to be within 4% of the expected values, and each is conserved to within 2% during the scattering processes.

Figure 1 shows the time evolution, integrated over the coordinate perpendicular to the figure, of the baryon

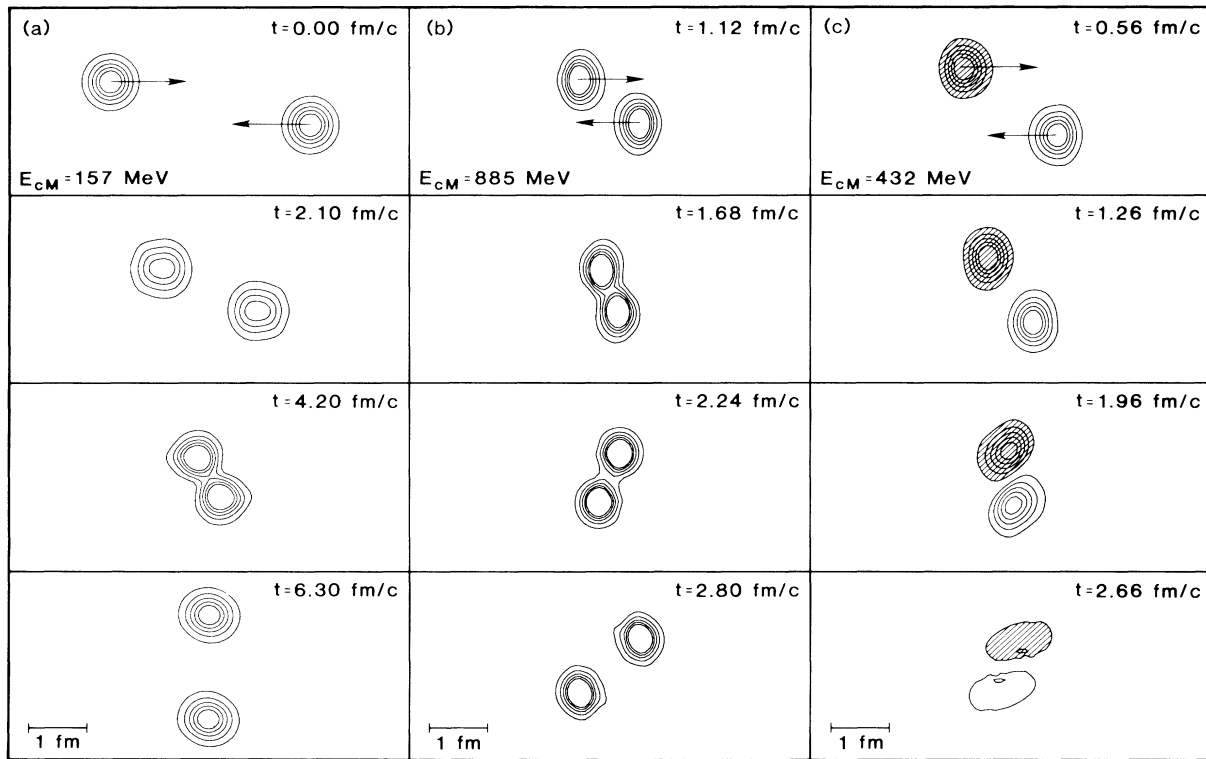


FIG. 1. The time evolution of the baryon density, in the c.m. frame, (a),(b) for SS collisions and (c) for $S\bar{S}$ annihilation. Equally spaced contours are shown, and the negative baryon density of the \bar{S} is shaded.

density for two skyrmion-skyrmion (SS) collisions at impact parameter $b=0.8$ fm. The center-of-mass velocities of the individual skyrmions in these cases are $v=0.4c$ and $0.75c$ ($E_{c.m.}=157$ and 885 MeV, respectively). The lower-energy SS collision demonstrates the importance of the three dimensions; the originally spherical solitons scatter in a direction roughly perpendicular to their initial motion. The outgoing skyrmions are distorted by the interaction, which results in a loss of kinetic energy of relative motion. In the higher-energy SS collision, the relativistic contraction of the skyrmions is clearly visible ($\gamma \approx 1.5$) and the inelasticity in the collision has increased (see below). Comparison of these two $b=0.8$ -fm events shows that the scattering angle θ decreases dramatically with increased bombarding energy, from $\theta \approx 90^\circ$ at $v=0.4c$ to $\theta \approx 10^\circ$ at $v=0.75c$; skyrmions become rather transparent at high energies.

Also shown in Fig. 1 is a skyrmion-antiskyrmion ($S\bar{S}$) collision at $b=1.2$ fm and $v=0.6c$ ($E_{c.m.}=432$ MeV). We construct the initial antiskyrmion by inverting the hedgehog's pion field and then rotating it by 180° around the axis parallel to the line of motion. The potential energy of the $S\bar{S}$ system decreases and the kinetic energy increases in the course of this annihilation until the rapid variation of the chiral fields leads to a failure of the numerical integration. We plan to study this pro-

cess further as a function of impact parameter and will attempt to extract the $S\bar{S}$ annihilation cross section.

Figure 2 is a more detailed presentation of a collision at $b=0.4$ fm and $v=0.4c$ ($E_{c.m.}=157$ MeV). This is a nearly central collision, which is expected to probe the "hard core" of the SS interaction; the scattering angle is approximately 125° . Note that initially not all momentum density vectors of the moving skyrmion point in the direction of motion because of nonvanishing spatial components of the stress tensor for a skyrmion at rest. In the final stages of the event, pion waves are emitted from the skyrmions, as is indicated by the presence of a nonvanishing pion field and momentum density in regions of zero baryon density. A vortex structure can be seen in the momentum density in the third frame of the sequence, and a small rotation of the pion field in each final-state skyrmion is visible, indicating rotational motion as a result of the collision.

A succinct measure of the collision dynamics is the baryon separation coordinate,

$$\mathbf{R}(t) = \mathbf{n} \int d^3r |\mathbf{n} \cdot \mathbf{r}| \rho_B(\mathbf{r}, t). \quad (4)$$

Here \mathbf{r} is measured from the center of mass, ρ_B is the baryon density, and \mathbf{n} is the direction in the scattering plane of the principal axis of the baryon inertia tensor

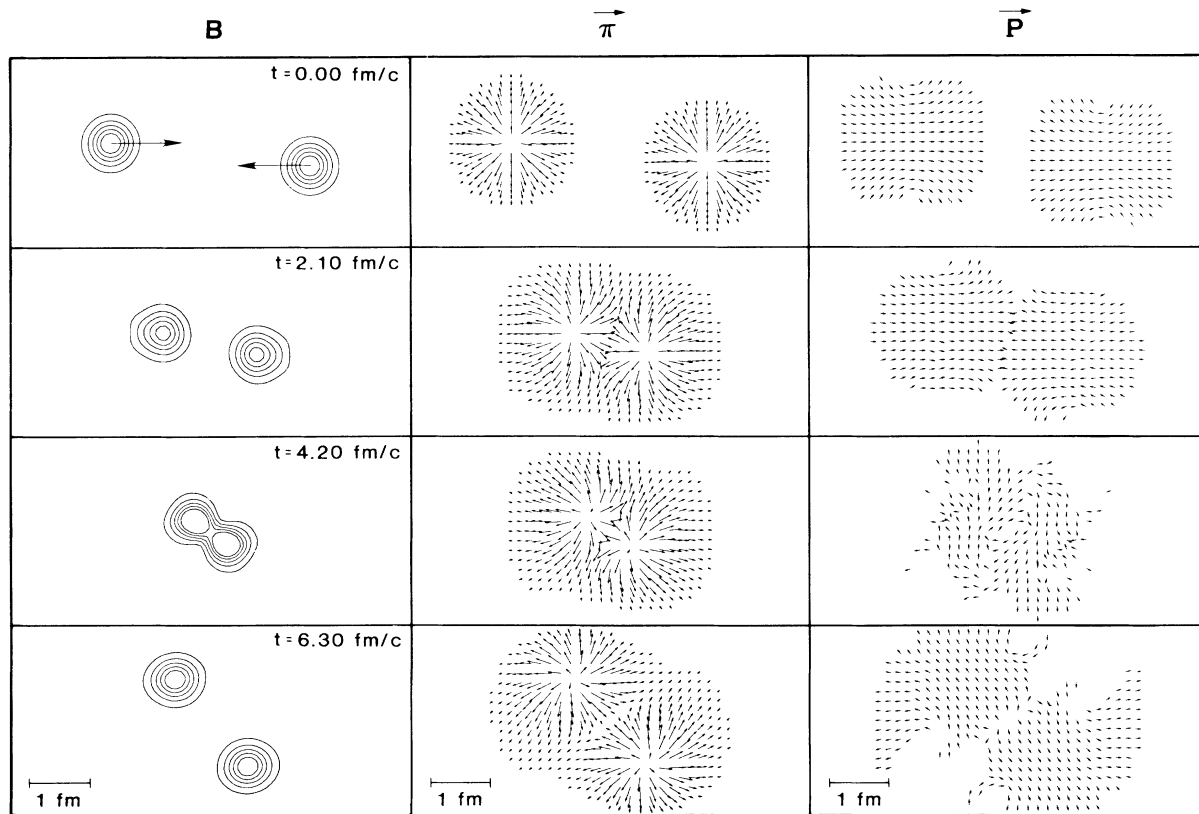


FIG. 2. The time evolution of the baryon density, B , isovector pion field in the collision plane, Π , and momentum density, \mathbf{P} , for a SS collision at $v=0.4c$ and $b=0.4$ fm. The density of points shown is one quarter of the density of our lattice. Each arrow represents the value of the pion field or direction of the momentum density at its tail.

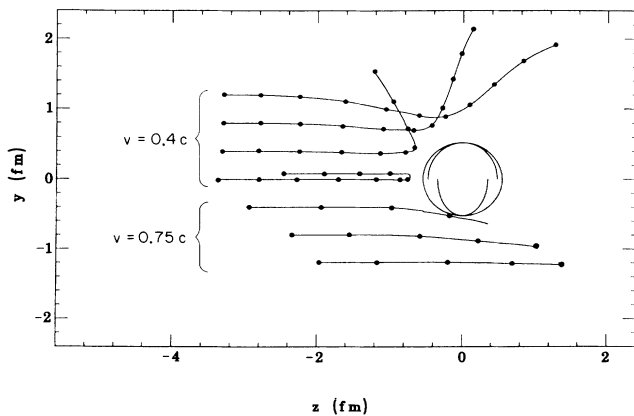


FIG. 3. The baryon separation coordinate $\mathbf{R}(t)$. We plot trajectories for $b=0.4, 0.8,$ and 1.2 fm at $v=0.4c$ and $v=0.75c$, and for $b=0.0$ fm at $v=0.4c$. Dots indicate time intervals of 0.70 fm/c. The path of the outgoing skyrmion for $b=0$ has been displaced slightly. The radius of the circle is calculated by evaluation of Eq. (4) for a spherically symmetric skyrmion with baryon number 1. It shows the minimum value of R expected if the skyrmions interpenetrated without distortion, while the ellipses show the effects of Lorentz contraction.

having the smaller eigenvalue. In Fig. 3 we give the trajectories of $\mathbf{R}(t)$ for various SS collisions. The systematics of the trajectories are generally as expected, with the short-distance repulsion causing a bouncing at small impact parameters that evolves toward a gentle forward deflection in more peripheral collisions. From the behavior of $\mathbf{R}(t)$ after the collision, we can extract the final velocity, v_f , and deflection angle, θ , of each skyrmion. In Fig. 4, we summarize our results for the deflection function $\theta(b)$ and the inelasticity $v_f(b)/v$. As mentioned earlier, the energy dependence of $\theta(b)$ is pronounced. The inelasticity approaches unity at large impact parameters but is less than 1 at smaller impact parameters (except for the $b=0$ collision, which appears to be elastic). It assumes its smallest values in collisions with intermediate impact parameters, where rotational modes can be excited in addition to vibrational motion.

In summary, we have presented the first numerical solutions of the (3+1)-dimensional classical field equations describing baryon-baryon collisions in the Skyrme model. We have made a preliminary investigation of the character of the collisions for $E_{c.m.} \leq 885$ MeV and have extracted the inelasticity and scattering angle at various

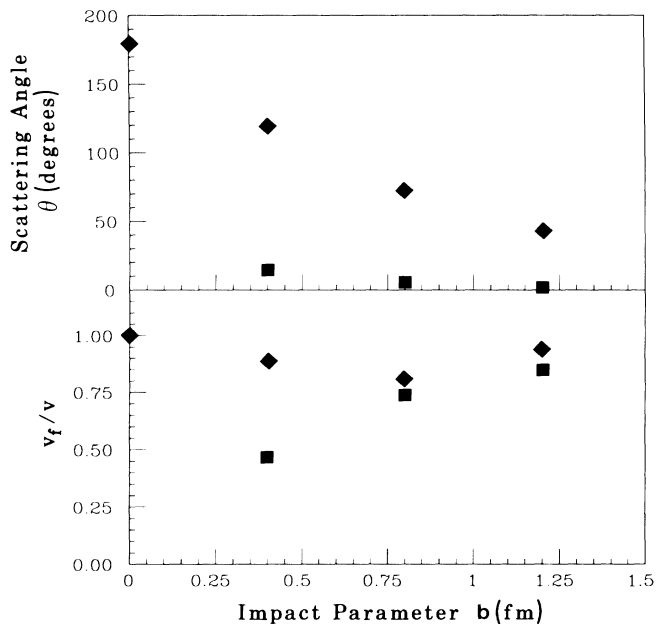


FIG. 4. The dependence of the scattering angle and inelasticity on the impact parameter. Diamonds and squares represent $v = 0.4c$ and $0.75c$ collisions, respectively.

impact parameters. We have also demonstrated baryon-antibaryon annihilation at nonzero impact parameters. More refined and systematic studies along these lines offer a number of interesting possibilities, including a calculation of the differential NN and $N\bar{N}$ elastic cross sections, together with the $N\bar{N}$ annihilation cross section, an analysis of the time dependence of the interbaryon separation to determine an effective potential, a quanti-

tative comparison of the adiabatic and dynamic field configurations, and a calculation of cross sections for baryon resonance and meson production.

Our calculations have been carried out under the auspices of both the U.S. Department of Energy (National Magnetic Fusion Energy Computer Center at Lawrence Livermore Laboratory) and National Science Foundation (San Diego Supercomputer Center). One of us (H.M.S.) acknowledges the support of the computing center at the National Science Foundation Institute of Theoretical Physics in Santa Barbara, CA. This work has been supported by the National Science Foundation under Grants No. PHY85-05682 and No. PHY86-04197 at Caltech, and Grants No. PHY86-11103 and No. PHY87-06748 at Westmont College, and by U.S. Department of Energy under Contract No. DE-FG03-87ER40347 at California State University, Northridge.

^(a)Also Department of Physics and Astronomy, California State University, Northridge, CA 91330.

^(b)Also Department of Physics, Westmont College, Santa Barbara, CA 93106.

¹I. Zahed and G. E. Brown, Phys. Rep. **142**, 1 (1986); T. H. R. Skyrme, Proc. Roy. Soc. London A **260**, 127 (1961), and Nucl. Phys. **31**, 5506 (1962); G. S. Adkins, C. R. Nappi, and E. Witten, Nucl. Phys. **B228**, 552 (1983).

²H. M. Sommermann, H. W. Wyld, and C. J. Pethick, Phys. Rev. Lett. **55**, 476 (1985); J. J. M. Verbaarschot, University of Illinois Report No. ILL-(TH)-87-13, 1987 (to be published); V. B. Kopeliovich and B. E. Shtern, JETP Lett. **45**, 203 (1987).

³J. J. M. Verbaarschot, T. S. Walhout, J. Wambach, and H. W. Wyld, Nucl. Phys. **A461**, 603 (1987).